Model and Simulation of an Ion Exchange Process for the Extraction of Antimony

Gerardo Cifuentes*[1], Jaime Simpson[1], Cesar Zúñiga[2], Leoncio Briones[3], Alejandro Morales[4]

[1]Departamento de Ingeniería Metalúrgica, Facultad de Ingeniería, Universidad de Santiago de Chile, Avenida Libertador Bernardo O'Higgins 3363, Casilla 10233, Fono: 56-2-7183224, Santiago, Chile
[2]Departamento de Ingeniería Química, Facultad de Ingeniería, Universidad de Santiago de Chile, Santiago, Chile
[3]Departamento de Ingeniería Mecánica, Facultad de Ingeniería, Universidad de Santiago de Chile, Santiago, Chile
[4]Departamento de Ingeniería Metalúrgica, Universidad Católica del Norte, Avenida Angamos 0610, Antofagasta, Chile
*gerardo.cifuentes@usach.cl

***Abstract*- In this paper a model is proposed for the removal of Sb by ion exchange from copper refining electrolytes. The correction factors for the MX-2, UR-3300S and Duolite C-467 resins were 0.5531, 0.2839 and 0.5455, respectively, and the model's average percentage error was 3.01%.**

Keywords- Antimony; IX; Modeling; Copper; Electrorefining

I. INTRODUCTION

In the processes for obtaining de copper by pyrometallurgy, a fundamental stage is the electrorefining of impure copper anodes (98-99.8% de Cu). In this stage by applying a potential difference, the copper present in the anode is dissolved electrochemically in the electrolytic solution, and is deposited on a stainless steel or pure copper cathode. At the same time, some of the impurities contained in the anode (As, Sb, Bi, S, Fe, Zn, Ni, Co) are dissolved in the electrolytic solution and the rest of those impurities (Ag, Se, Te, Pb) do not go into the solution and precipitate as "anode slime". In turn, as a result of matter transfer mechanisms, physical contamination of the pure copper cathodes occurs (occlusion of solids), affecting the electric properties of the copper and the quality of the pure copper cathodes [1].

Control of the impurities presenting in the electrolyte is done mainly by purging the electrolytic solution. However, the impurities that have the greatest incidence on cathode contamination and on operational problems are As and Sb compounds. There is a known ratio between arsenic and antimony (As/Sb $\geq$ 2) that prevents the formation of floating slime that can cause physical contamination of the pure copper cathode, leading to an As and Sb solubility curve from which it can be concluded that as the arsenic in solution increases, the solubility of antimony decreases. However, increased Sb in copper sulfide ores and its concentration in the electrolytic solution in spite of keeping the (As/Sb $\geq$2) causes this Sb "equilibrium" difference to form a compound (Sb_2O_3) that precipitates throughout the system, clogging ducts and physically contaminating the cathodes.

This situation has made refineries take short-term measures to remove the excess antimony. Considering the above and reviewing the literature, there is a large variety of publications that highlight the benefits of using ion exchange resins to remove the antimony present in the electrolyte of copper refineries, particularly the work of Dreissinger and Sasaki [2, 3]. Industrially, this ion exchange process has been studied on the pilot scale in the Tamano [4], Nippon Hitachi, Saganoseki, Noranda, and other refineries.

Chile studies have been made [5] and are continuing at both the laboratory and pilot scales of ion exchange plants aimed at defining parameters for designing ion exchange plants at the industrial scale for extracting antimony. In view of the economic perspectives of the ion exchange techniques in mining as such and of their repercussion on the quality of the copper cathodes, it is of interest for the design and control of the process (control of flow, height of bed, initial solute concentration, etc.) to have a model and simulation of the ion exchange process.

A. Basics of Ion Exchange Resins

Ion exchange operations are mainly substitution chemical reactions of an ion in solution by another in the insoluble resin. The mechanisms of these reactions and the techniques used to carry them out are similar to those of adsorption, and in most practical engineering cases, ion exchange is considered as a special case of adsorption.

As in previous studies, the same as in adsorption, it is necessary to determine a mechanism that will control the ion exchange process for practical design purposes. Thus, it is found that the rate at which the ion exchange takeing place depends (the same as adsorption) on the following transport phenomena that occur as the ion exchange progresses [4]:

1. diffusion of ions from the fluid to the outer surface of the resin;
2. internal diffusion of ions through the solid to the exchange site;
3. ion exchange;
4. external diffusion of the released ions to the surface of the solid.

When the ion exchange reactions are fast compared to the rate of mass transfer, the design methods developed for traditional adsorbers can be applied directly to the ion exchange operations.

B. Breakthrough Curve

The continuous path of a concentrated solution with an element of interest (Sb) through a fixed bed (porous) of

resin behaves in a way that can be described as follows, where BV are the Bed Volume Flow of the solution [4]).

The solution of concentration C_0 comes in contact with the upper part of the resin bed, extracting practically all the solute, and the remainder is extracted in the lower part of the bed, ideally getting a solution free of solute, as shown in Part a) of Fig. 1.

As the solution continues flowing, the extraction zone is displaced downward (Part b) of Fig. 1) as a wave. The bed is half saturated and the concentration of the outgoing solution is still practically zero (C_b).

Part c) of Fig. 1 shows that the extraction zone has reached the bottom of the bed and the solute concentration in the effluent has increased suddenly to a considerable value C_c. For the first time, it is said that the system has reached the "breaking point". Now the outgoing concentration increases rapidly as it goes past the extraction zone through the bottom of the bed.

In Zone d) the outgoing concentration C_d is practically C_0, the extraction zone has touched the bottom of the bed, and the resin is completely saturated.

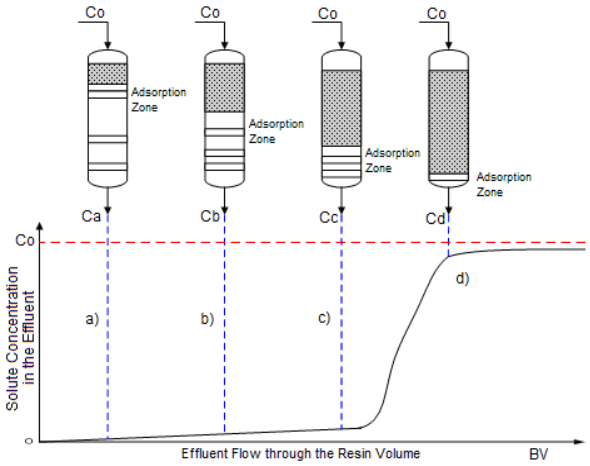

Fig. 1 Breakthrough Curve

II. EXPERIMENTAL PART

To obtain the model is necessary conceptually solve the mechanisms of mass transfer and the mass balance together, all these considerations are mentioned and represented by their respective equations upon the following pages of this work.

The mass transfer produced between a boundary surface and a moving fluid, or between two relatively immiscible fluids in motion, is known as mass transfer by convection, and it takes place in the direction in which solute concentration is decreasing, and this process is similar to the convective heat transfer mechanism [7], which is based on the double film layer theory of mass transfer. The rate based on this theory can be formulated considering the case in which a fluid passes through a fixed adsorbent bed. Assuming that the concentration is constant in the direction perpendicular to the fluid's (L subscript) direction (radial direction), the concentration profile of solute (S subscript) "i" can be interpreted by means of Fig. 2.

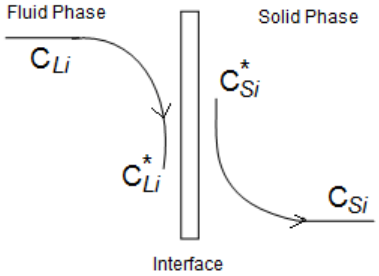

Fig. 2 Interface mass transfer profile

According to Fig. 2 and keeping in mind the analogies with heat transfer, the following can be inferred.

The rate equation corresponding to the mass transfer of component "i" from the body of the fluid to the interface zone (transfer zone) is represented by [7]

$$N_{Li} = k_{Li} \cdot A_L \cdot \left(C_{Li} - C_{Li}^{\ *}\right) \tag{2.1}$$

where:

N_{Li} : number of moles transferred per unit time and unit volume of empty bed.

A_L : interface area between the fluid phase and the solid phase per unit volume of empty column.

k_{Li} : mass transfer coefficient, volume of empty column per unit time and unit interfacial area.

C_{Li} : solute concentration in the body of the fluid phase, moles per unit empty volume (free volume between the resins).

C^*_{Li} : solute concentration in the interface (equilibrium concentration).

The rate of mass transfer of solute "i" from the interface to the solid phase is given by [5].

$$N_{Si} = k_{Si} \cdot A_S \cdot \left(C_{Si}^{\ *} - C_{Si}\right) \tag{2.2}$$

where:

N_{Si} : number of moles transferred per unit time and unit volume of resin.

A_S : interface area between the fluid phase and the solid phase per unit volume of resin.

k_{Si} : mass transfer coefficient, resin volume per unit time and unit interface area.

C_{Si} : solute concentration in the solid phase per unit volume of resin.

Defining the porosity of the resin bed as

$$\varepsilon = \frac{volume\ \ of\ \ spaces\ \ between\ \ resins}{volume\ \ of\ \ bed}$$

$$1 - \varepsilon = \frac{resin\ volume}{bed\ \ volume} \tag{2.3}$$

we have

$$A_s = \frac{A_L}{1-\varepsilon} \tag{2.4}$$

$$N_{Si} = \left(\frac{1}{1-\varepsilon}\right)\cdot N_{Li} \tag{2.5}$$

Substituting Equations (2.1) and (2.2) in (2.5) we get

$$N_{Si} = k_{Si}\cdot A_S \cdot \left(C^*_{Si} - C_{Si}\right) = \frac{k_{Li}\cdot A_L \cdot \left(C_{Li} - C^*_{Li}\right)}{1-\varepsilon} \tag{2.6}$$

A. Mass Balance in the Solid Phase

Making a mass balance of the fixed bed ion exchange column with cross sectional area *S* and under the following assumptions:

- concentration is constant in the radial direction (direction perpendicular to flow);
- the concentration gradients within the solid are negligible;
- mass transfer by diffusion is negligible;
- mass balance by diffusion is disregarded;

the mass balance over solute "i" in the adsorbed (solid) phase in a volume element $S{\cdot}dz$ is given by (see Fig. 3):

$$Input - Output = Accumulation - Generation \tag{3.1}$$

where:

$$Input = (1-\varepsilon)\cdot N_{Si}\cdot S{\cdot}dz$$

$$Output = 0$$

$$Generation = 0$$

$$Accumulation = \frac{\partial}{\partial t}\left[(1-\varepsilon)\cdot C_{Si}\cdot S{\cdot}dz\right]$$

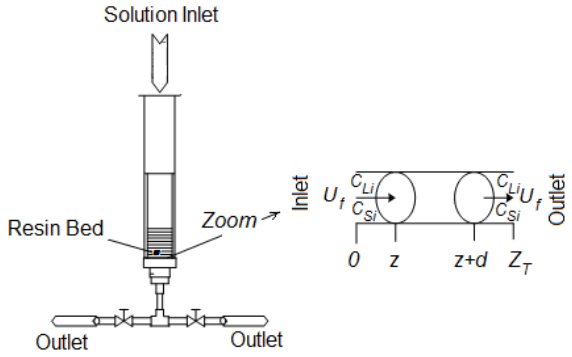

Fig. 3 Schematic diagram of a fixed bed column

Replacing in Equation (3.1) and arranging algebraically:

$$N_{Si} = \frac{\partial C_{Si}}{\partial t} \tag{3.2}$$

Then, equating Equation (2.6) with (3.2):

$$\frac{\partial C_{Si}}{\partial t} = \frac{k_{Li}\cdot A_L}{(1-\varepsilon)}\cdot\left(C_{Li} - C^*_{Li}\right) \tag{3.3}$$

B. Mass Balance in the Liquid Phase

Making a mass balance according to Equation (2.2) and with the following assumptions:

- solute concentration "i" (Sb in this case) in the fluid phase is constant in all the fluid's directions;

- the rate of mass transfer by diffusion in the fluid phase is negligible in all directions;

- the linear velocity U_f of the fluid phase is constant.

The mass balance over solute "i" in the fluid phase in a volume element $S{\cdot}dz$ is presented in Fig. 3.

Where

$$Input = U_f\cdot\varepsilon\cdot S\cdot C_{Li}\,|_z$$

$$Output = U_f\cdot\varepsilon\cdot S\cdot C_{Li}\,|_{z+dz} \quad + \quad N_{Si}\cdot(1-\varepsilon)\cdot S{\cdot}dz$$

$$Generation = 0$$

$$Accumulation = \frac{\partial}{\partial t}\left(\varepsilon\cdot C_{Li}\cdot S{\cdot}dz\right)$$

Replacing in Equation (3.1) and since U_f, ε and S are independent of time and position, and applying the definition of derivative and taking the limit at which dz tends to zero, we have

$$-U_f\frac{\partial C_{Li}}{\partial z} - \frac{(1-\varepsilon)}{\varepsilon}\cdot N_{si} = \frac{\partial C_{Li}}{\partial t} \tag{3.4}$$

Replacing Equation (2.6) in (3.4), we have

$$-U_f\frac{\partial C_{Li}}{\partial z} - \frac{k_{Li}\cdot A_L}{\varepsilon}\cdot\left(C_{Li} - C^*_{Li}\right) = \frac{\partial C_{Li}}{\partial t} \tag{3.5}$$

Therefore, we see that the mathematical modeling of the system is determined by two differential equations in partial derivatives[6]:

$$\frac{\partial C_{Si}}{\partial t} = \frac{k_{Li}\cdot A_L}{(1-\varepsilon)}\cdot\left(C_{Li} - C^*_{Li}\right) \tag{3.3}$$

$$-U_f\frac{\partial C_{Li}}{\partial z} - \frac{k_{Li}\cdot A_L}{\varepsilon}\cdot\left(C_{Li} - C^*_{Li}\right) = \frac{\partial C_{Li}}{\partial t} \tag{3.5}$$

C. Analytic Solution of the Model

According to the equations derived under Points 3.1 and 3.2, keeping in mind that we are working on an ideally isothermal system, assuming that perfect mixing occurs in the radial direction of the column, and that the electrolytic solution is displaced uniformly in the radial and longitudinal directions of the column, and considering also that the resistance offered by the solid to matter transfer is negligible, what we are trying to find is an equation that will predict the concentration of solute "i" (antimony) at the outlet of the column at any instant.

Thus, Equation (3.5) is simplified if a modified time variable is introduced [6]:

$$t^* = t - z\cdot\left(\frac{e\cdot S\cdot C_{L0}}{U_f}\right) \tag{3.6}$$

Equations (3.3) and (3.5) can be expressed in the following way:

$$\left(\frac{\partial C_{Si}}{\partial t^*}\right)_Z = \frac{(k_{la})_{Li}}{(1-\varepsilon)} \cdot \left(C_{Li} - C_L^*\right) \quad (3.7)$$

$$\left(\frac{\partial C_{Li}}{\partial z}\right)_{t^*} = -\frac{(k_{la})_{Li}}{U_f} \cdot \left(C_{Li} - C_{Li}^*\right) \quad (3.8)$$

Therefore, the boundary conditions (C_{L1} and C_{L2}) of the system of differential equations in partial derivatives are:

$$\begin{aligned} &C_{L1}: \quad for \quad t^* = 0 \quad C_{Si} = 0 \quad for\ all \quad z > 0 \\ &C_{L2}: \quad for \quad z = 0 \quad C_{Li} = C_{L0} \quad for\ all \quad t^* > 0 \end{aligned} \quad (3.9)$$

To solve this system of equations it is convenient to use the following change of nondimensional variables:

$$X = \frac{C_{Li}}{C_{L0}} \quad (3.10)$$

$$Y = \frac{m \cdot C_{Si}}{C_{L0}} \quad (3.11)$$

$$\xi = \frac{z \cdot S \cdot (k_{la})_{Li}}{U_f} \quad (3.12)$$

$$\tau = \frac{m \cdot t^* \cdot (k_{la})_{Li}}{1-\varepsilon} \quad (3.13)$$

where

C_{L0} = initial solute concentration in the fluid;
m = equilibrium isotherm constant;
z = height of the resin bed;
k_{la} = volumetric matter transfer coefficient.

Based on these variables, the differential equations and the boundary conditions are

$$\frac{\partial X}{\partial \xi} = -(X - Y) \quad (3.14)$$

$$\frac{\partial Y}{\partial \tau} = (X - Y) \quad (3.15)$$

$$\begin{aligned} &C_{L1}: \quad for \quad \tau = 0 \quad Y = 0 \quad for\ all\ values\ of \quad \xi \\ &C_{L2}: \quad for \quad \xi = 0 \quad X = 1 \quad for\ all\ values\ of \quad \tau \end{aligned} \quad (3.16)$$

whose solution is given by[8]

$$C_{Li}(t) = C_{L0} \cdot \left[1 - \int_0^{\xi} e^{-(\tau+\xi)} \cdot J_0\left(2i \cdot \sqrt{\xi \cdot \tau}\right) \cdot d\xi\right] \quad (3.17)$$

The solution described by Equation (3.17) has been modified empirically with the purpose of getting a more accurate response with respect to the behavior implied in the ion exchange process. So the equation that describes the concentration of solute "i" at the column outlet at any instant of time is given by

$$C_{Li}(t) = f_{correction} \cdot C_{L0} \cdot \left[1 - e^{\int_0^{\xi} e^{-(\xi+\tau)} \cdot J_0\left(2i \cdot \sqrt{\xi \cdot \tau}\right) d\xi}\right] \quad (3.18)$$

This equation was programmed in MATLAB® in order to generate the modeled and simulated breakthrough curve.

D. Experimental Validation

The experimental data used in this publication, Tables I and II, correspond to values determined in pilot experiments made with three different resins: MX-2, UR-3300S, and Duolite C-467. The electrolytic solution used came from an important refinery in the north of Chile.

TABLE I INITIAL CONCENTRATION OF THE ELECTROLYTIC SOLUTION

Sb [kg/m3]	Cu [kg/m3]	Fe [kg/m3]	As [kg/m3]	H^+ [g/L]
0.2167	39.4	0.174	9.76	220

TABLE II OUTGOING CONCENTRATION OF ANTIMONY IN THE ELECTROLYTE FOR EACH RESIN BED COLUMN ANALYZED

Resin	MX-2	UR-3300S	Duolite C-467
t [h]	Sb [kg/m3]	Sb [kg/m3]	Sb [kg/m3]
1	0.0296	0.0366	0.0398
2	0.1025	0.0544	0.1085
3	0.1071	0.0615	0.1170
4	0.1095	0.0616	0.1139
5	0.1195	0.0605	0.1175
6	0.1198	0.0611	0.1186
7	0.1201	0.0617	0.1191
8	0.1201	0.0619	0.1189

E. Experimental Breakthrough Curve

Fig. 4 shows the experimental breakthrough curves obtained for the following resins:

- Duolite C-467: red line;
-UR-3300S: green line;
-MX-2: blue line.

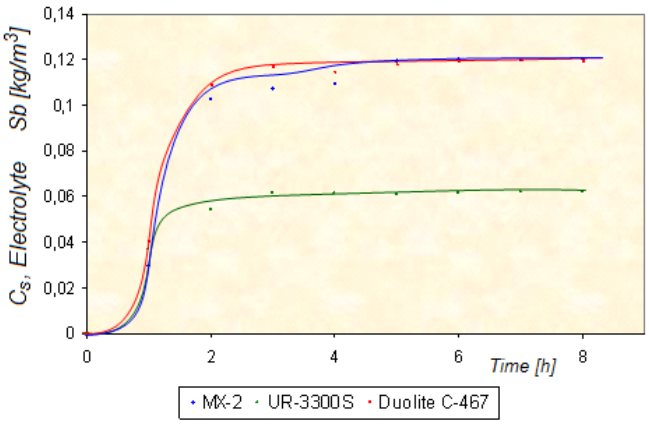

Fig. 4 Experimental breakthrough curves

To carry out this study, laboratory tests were conducted in order to characterize the behavior of three different ion exchange resins for the extraction of antimony, through continuous ion exchange in columns to obtain the breakthrough curves. The sequence of the test was: adsorption-1th washing—elution-2th washing, 10 cycles in total were tested.

The column used was glass of 14 mm diameter and 1.000 mm height, with heating jacket to maintain the operating temperature at 60°C. The filling of resin in the column was 700 mm high, equivalent to 0.108 L of volumen resin (*Vr*). The electrolyte used in this study was: Cu 37.50 g/L, H_2SO_4 204.05 g/L, As 8.50 g/L and Sb 0.21 g/L. Each cycle was performed with the following conditions: electrolyte flow 0.0166 L/min, total volume of electrolyte treated 4 L; the first wash was performed at 5 ml/min with a total of 0.4 L; the elution was performed using a tartaric acid solution of 33 g/L and potassium bitartrate 6 g/L, the flow rate was 5 ml/min with a total of 0.3 L; the second wash was performed under the same conditions as the first wash.

F. Modeled Breakthrough Curve

Fig. 5 shows the breakthrough curves (for each resin) modeled from Equation (3.18).

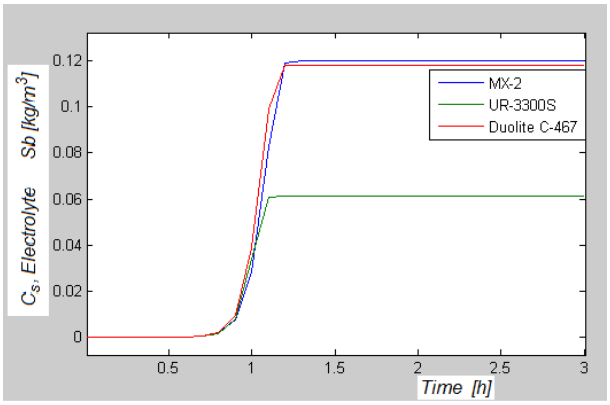

Fig. 5 Modeled breakthrough curves

Table III shows the correction factors and the error delivered by the proposed model, which are within the acceptability range (less than 10%)[9].

TABLE III CORRECTION FACTOR AND PERCENTAGE ERROR OBTAINED BY MEANS OF MODELING AND SIMULATION

Resin Bed	$f_{correction}$	% Error
MX-2	0.5531	3.72
UR-3300S	0.2839	2.94
Duolite C-467	0.5455	2.38

Table IV shows the volumetric matter transfer coefficients (k_{la}) for each resin bed, which were determined iteratively for each resin. From the k_{la} values it can be inferred that resin UR-3300S presents less resistance to matter transfer and greater antimony extraction capacity (at low k_{la} values there is greater resistance to matter transfer), while resins MX-2 and Duolite C-467 behave quite similarly in the ion exchange process.

TABLE IV VOLUMETRIC MATTER TRANSFER COEFFICIENT OF Sb ADSORPTION

Resin	k_{La} [kg/m3 h]
MX-2	0.0238
UR-3300S	0.0431
Duolite C-467	0.0257

G. Different Operating Scenarios

The behaviour of the breakthrough curves modelled for resin UR-3300S under different operating conditions is shown below.

In Fig. 6, it can see, as k_{la} increases ($k_{la1} < k_{la2} < k_{la3}$), leading to less resistance to matter transfer and a greater capacity for Sb extraction in less time, this is reflected in a decrease of breaking time and a displacement of the breakthrough curve to the left. These results are similar behavior to the experimental values in Table 4, from the k_{la} values it can be inferred that resin UR-3300S presents less resistance to matter transfer and greater antimony extraction capacity (at low k_{la} values there is greater resistance to matter transfer), while resins MX-2 and Duolite C-467 behave quite similarly in the ion exchange process.

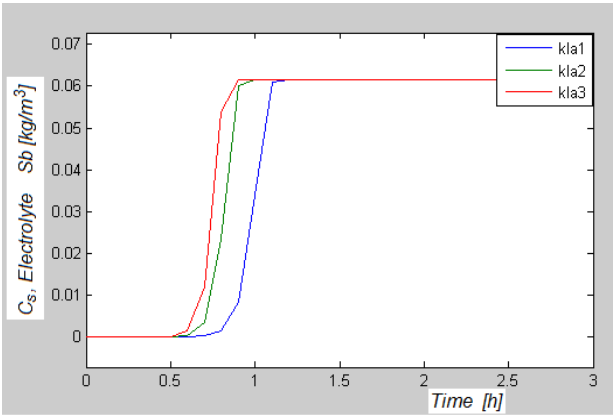

Fig. 6 Resin UR-3300S breakthrough curve modelled at different k_{la}

If maintained the constant diameter of the column, as Vr increases, there is an increase in height of the resin bed so that the liquid will move through a longer distance in the bed, losing a greater amount of Sb and therefore requires more time for the resin bed which is completely saturated. Therefore, the curve shifts to the right, thereby increasing the breaking time of the breakthrough curve in Fig. 7.

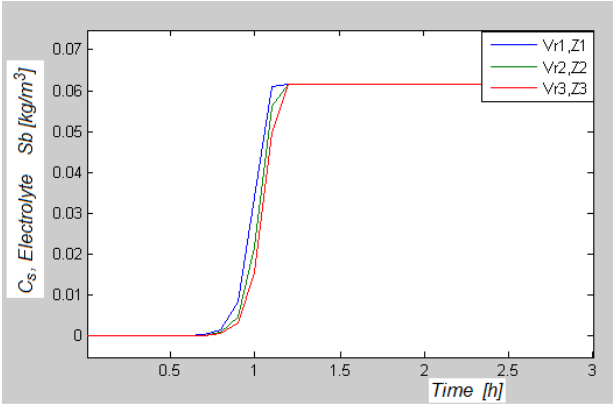

Fig. 7 Resin UR-3300S breakthrough curve modeled at different resin bed volumes (Vr)

In Figure 8 it was observed that, with increasing the initial concentration of antimony (CSb1<CSb2<CSb3) in the feed solution, was increased the capture kinetics of antimony, this reflected in the leftward shift of the breakthrough curve.

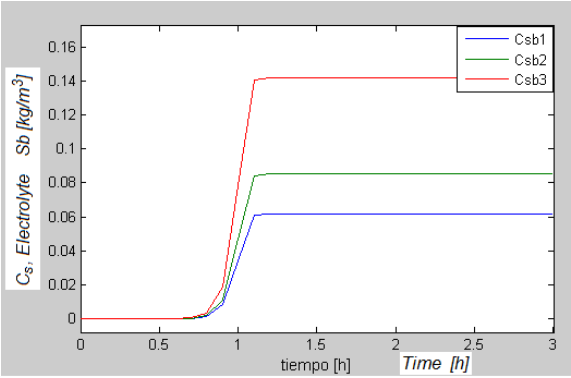

Fig. 8 Resin UR-3300S breakthrough curve modeled at different initial Sb concentrations, C_{Sb}

TABLE V VALUES SIMULATED ON THE MODEL

UR-3300S	k_{la} [kg/m3h]	Vr [m3]	C_{Sb} [kg/m3]
1	0.0431	0.0001078	0.2167
2	0.0517	0.0002	0.3
3	0.0560	0.0003	0.5

III. CONCLUSIONS

It is possible to conclude that the proposed model that describes the ion exchange process in a fixed bed column is representative of the process and agrees with the experimental data given in the available literature. From what has been presented here, it is inferred that the volumetric matter transfer coefficients are a fitting approximation of the ion exchange process and they are the ones that have a major incidence in the process.

It is also possible to generate operating scenarios by means of the proposed model and its programming in MATLAB®, getting satisfactory results in agreement with what is predicted by the literature, namely:

As k_{la} increases (Fig. 6), leading to less resistance to matter transfer and a greater capacity for Sb extraction in less time, this is reflected in a decrease of breaking time and a displacement of the breakthrough curve to the left.

As Vr increases (Fig. 7), keeping the column diameter constant, there is an increase in the height of the resin bed, so the fluid will travel through a longer distance in the bed, losing a greater amount of Sb and therefore requiring more time for the resin bed to become completely saturated. Therefore the curve will be displaced to the right, thereby increasing the breaking time of the breakthrough curve.

Due to the increase of the input concentration of Sb in the electrolyte (Fig. 8), the breakthough curve becomes slightly more pronounced and breakage time decreases slightly.

ACKNOWLEDGEMENTS

The authors acknowledge the support of DICYT of the Universidad de Santiago de Chile, Usach

REFERENCES

[1] K. Biswas, W.G. Davenport, Extractive Metallurgy of Copper; fourth edition, Elsevier Science, (2002).

[2] D. Dreissinger and B. J. Y. Scholey, “Ion Exchange Removal of Sb and Bi from Copper Electrolytes” in Procs. Copper 1995, Vol III, The Met. Soc. of CIM., 1995, 305-314.

[3] Y. Sasaki, S. Kaway, Y. Takasawa and S. Furuga. “Development of Antimony Removal Process for Copper Electrolyte", in Proceeding of Copper 91, Vol III, Pergamon Press, Elmsford, N.Y., USA, 1991, 245-254.

[4] T. Shibata, M. Hashiuchi and T. Kato. “Tamano Refinery’s New Process for Removing Impurities from Electrolyte”, in Proceeding of The Electrorefinning and Winning of Copper,. TMS-AIME, Warrendale, P.A., 1987, 99-116.

[5] Román E.A., Guzmán J.E., Muto S. “Antimony removal by ion exchange in a Chilean tankhouse at the pilot plant scale” in Proceeding of. Copper 1999, Vol III, The Minerals, Metals & Materials Society, 1999, 225-236.

[6] Treybal E. Robert; Operaciones de Transferencia de Masa; second edition, Mc Graw-Hill, Mexico, (1988).

[7] Welty James R., Charles E. Wicks, Fundamentos de Transferencia de Momento, Calor y Masa, second edition, Editorial Limusa, Mexico, (2001).

[8] Bird Byron R., Stewart E. Warren, Lightfoot N. Edwin, Fenómenos de Transporte; Un estudio sistemático de los fundamentos del transporte de materia, energía y cantidad de movimiento, first edition, Reverté S.A., Spain, (1992).

[9] Montgomery D.C., Runger G. C., Probabilidad y Estadística Aplicada a la Ingeniería, second edition, Ed. Limusa Wiley, Mexico, (2002).

Dr. Gerardo Cifuentes is Metallurgical Engineer since 1986 and graduated from M.Cs. and Dr.Cs. in Metallurgical Engineering at the University of Concepcion, Chile, in 1990 and 1998 respectively. His doctoral studies were conducted at the University of Concepcion and at the Technical University of Berlin, Germany. He is currently Professor in the Department of Metallurgical Engineering, University of Santiago of Chile (USACH) and participated in the programs of the Graduate School of Engineering at the same university with lines of research in the field of Electrometallurgy, Corrosion and Treatment of liquid effluents.